Pergamon

Available online at www.sciencedirect.com
SCIENCE DIRECT®

Cement and Concrete Research 33 (2003) 1669–1673

CEMENT AND CONCRETE RESEARCH

A strain-softening model for steel–concrete bond

Xiaohui Wang*, Xila Liu

Department of Civil Engineering, SJTU, Minhang, Shanghai 200240, PR China

Received 9 October 2002; accepted 10 April 2003

Abstract

A new analytical model is proposed to describe the bond strength between a ribbed reinforcement bar and concrete. The model is based on the partly cracked solution of a thick-walled cylinder exposed to radial internal pressure. Instead of considering the minimum crack number in previous solutions, smeared cracking and average stress–strain of concrete in tension are used in radial direction to describe the softening behavior of concrete. The results are compared with Tepfers' classic solutions and other previous solutions.

Keywords: Bond strength; Concrete; Smeared cracking; Softening

1. Introduction

The bond between steel and concrete consists of three mechanisms: adhesion, friction and mechanical interlock. The effect of chemical adhesion is small and friction forces do not develop until adhesion has failed and relative displacement between reinforcement bar and concrete occurs. Both mechanisms are important in the case of plain bars. For deformed bars, the mechanical interlock of the ribs of the bars embedded in concrete governs the bond stress-deformation behavior.

When bond failure is approached, transfer of force between a ribbed bar and concrete is achieved by the bearing of the ribs on the concrete. The resultant compressive forces are exerted by the ribs, which spread into the surrounding concrete at a certain angle. These inclined forces create circumferential tension forces in the concrete around the bar. If these tensile forces exceed the tensile capacity of concrete, splitting failures occur.

This problem is treated analytically by Tepfers [1] as a thick-walled cylinder subjected to internal radial pressure. The inner radius is determined by bar size, while the outer radius of the cylinder is determined by the smallest available dimension, which is usually given by the least thickness of the concrete cover. The radial pressure p of the bond stresses is balanced by tangential tensile stresses in the concrete (Fig. 1). In the plane of the bar, the radial pressure p is coupled to concrete bond stress τ along the surface of the bar by the assumption of a Mohr–Coulomb failure criterion. If the initial cohesion is disregarded and a wedge angle α is defined in Fig. 1, then

$$p = \tau \tan\alpha \qquad (1)$$

where the angle α is often set to 45°, so $p = \tau$.

To determine the cracking resistance, three stages are considered [1]: an uncracked elastic stage (lower bound), an uncracked plastic stage (upper bound) and an intermediate partly cracked elastic stage. The elastic stage gives the load when cracking starts from the bond surface between the concrete and the steel, and the partly cracked elastic stage gives the load when the longitudinal crack goes right through the concrete cover. Considering the plastic deformation of concrete, the final carrying capacity lies in between the partly cracked elastic stage and the plastic stage.

Since then, several research works [2–7] have been carried out on the basis of the idea of Tepfers. In order to consider the softening behavior of the concrete after cracking, the thick-walled cylinder is divided into two parts: an uncracked outer part and a partly cracked inner part. Different concrete tensile softening models are selected in the inner part, such as a power-law model and an exponential softening curve used by Reinhardt and Van der Veen [2], a linear-softening curve chosen by Olofsson et al. [3] and Noghabai [4] and an elastocohesive model proposed by Gambarova et al. [5] and Gambarova

* Corresponding author.
E-mail address: w_xiaoh@163.com (X. Wang).

0008-8846/03/$ – see front matter © 2003 Elsevier Ltd. All rights reserved.
doi:10.1016/S0008-8846(03)00137-6

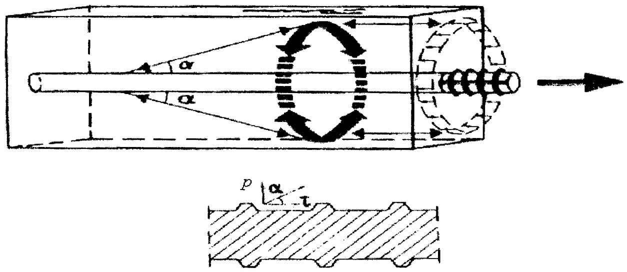

Fig. 1. Radial components of the bond forces are balanced against tensile stress rings in the concrete in an anchorage zone [1].

and Rosati [6]. However, these models have a common characteristic: they are related to the number of radial cracks. Therefore, the results of the problem are associated with the number of radial cracks. However, it is difficult to determine the number of cracks in real concrete structures because there are thousands of microcracks and cracks in cracked concrete.

In this article, based on the same methodology as mentioned above, an analytical model is proposed. Smeared cracking is assumed to form in the radial direction of the partly cracked inner part as tangential stresses exceed the tensile capacity of concrete. Therefore, the average stress–strain curve of concrete in tension is used and the average tangential tensile strain, integrated over the perimeter, represents the sum of the true, discrete crack openings. The assumption of constant radial displacement is adopted. The results are compared with Tepfers' solutions and other previous solutions.

2. A strain-softening model for bond strength

The methodology proposed by Tepfers [1] is also used. The problem of determining the maximum internal radial pressure p or maximum bond stress is divided into two parts; see Fig. 2, wherein the steel of radius R_0 is embedded in concrete with outer radius R_c, the concrete cover dimension measured from the center of the bar to the nearest surface of concrete. R_i defines the crack front, where the tangential stresses equal to the tensile strength of concrete f_{ct}.

For elastic outer part, boundary condition is used to obtain p_i (see Fig. 2b). The radial and tangential stresses are given by using the classic theory of elasticity:

$$\sigma_r = -p_i \frac{\frac{R_c^2}{r^2} - 1}{\frac{R_c^2}{R_i^2} - 1} \qquad \sigma_t = p_i \frac{\frac{R_c^2}{r^2} + 1}{\frac{R_c^2}{R_i^2} - 1} \tag{2}$$

Setting $\sigma_t|_{r=R_i} = f_{ct}$, p_i is given by

$$p_i = f_{ct} \frac{R_c^2 - R_i^2}{R_c^2 + R_i^2} \tag{3}$$

For the inner part, the displacement and stresses are considered. In order to describe the softening behavior of concrete, smeared cracks are assumed to form in the radial direction as tangential stresses exceed the tensile capacity of concrete f_{ct}; therefore, the formulation is written in terms of average stresses and strains, and the average tangential tensile strain ε_t, integrated over the perimeter, represents the sum of the true, discrete crack openings [8]. As a result, the total tangential elongation δ_t at a radial distance r, which is expressed as the sum of n crack widths plus the linear-elastic extension of the concrete between the cracks [2–7], can be expressed as:

$$\delta_t = 2\pi r \varepsilon_t \tag{4}$$

At a radial distance R_i, the tensile strength of concrete f_{ct} is reached and no cracks exist. Then, the total tangential elongation is

$$\delta_t = 2\pi R_i \varepsilon_t \approx 2\pi R_i \frac{f_{ct}}{E_0} = 2\pi R_i \varepsilon_{ct} \tag{5}$$

where the Poisson's effect is neglected in Eq. (5) [2–7]. E_0 is the initial elastic modulus of concrete and ε_{ct} is the tensile strain capacity of concrete, $\varepsilon_{ct} = f_{ct}/E_0$.

The associated radial displacement $u_r = R_i \varepsilon_{ct}$ is assumed to be constant [2–6]. Considering the compatibility between

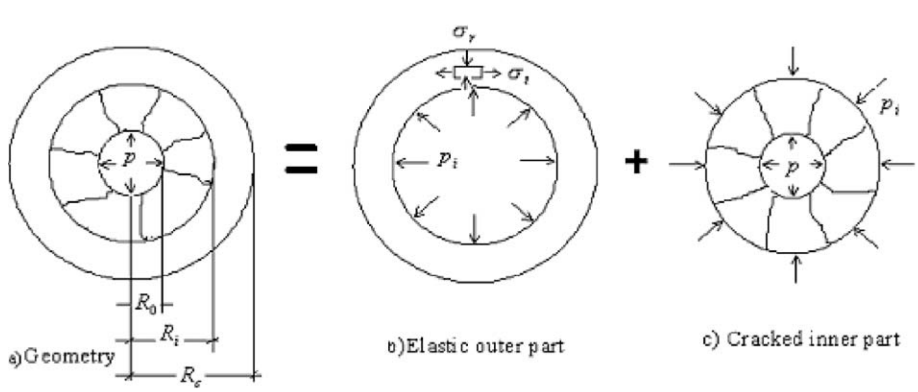

Fig. 2. Bond model for partly cracked concrete cylinder.

the cracked and the uncracked parts, the following equation can be obtained:

$$\delta_t = 2\pi r \varepsilon_t = 2\pi R_i \varepsilon_{ct} \tag{6}$$

Thus, the average tangential strain ε_t at a radial distance r is given by

$$\varepsilon_t = \frac{R_i}{r}\varepsilon_{ct} \tag{7}$$

In Eq. (7), ε_t is related to the constitutive relation of concrete in tension. The following stress–strain relationship of concrete in tension is used [8] (see Fig. 3):

$$\sigma_t = E_0\varepsilon_t \qquad \varepsilon_t \le \varepsilon_{ct} \tag{8-1}$$

$$\sigma_t = f_{ct}\left[1 - \frac{0.85(\varepsilon_t - \varepsilon_{ct})}{\varepsilon_1 - \varepsilon_{ct}}\right] \qquad \varepsilon_{ct} < \varepsilon_t \le \varepsilon_1 \tag{8-2}$$

$$\sigma_t = 0.15 f_{ct}\frac{\varepsilon_u - \varepsilon_t}{\varepsilon_u - \varepsilon_1} \qquad \varepsilon_1 < \varepsilon_t \le \varepsilon_u \tag{8-3}$$

where cracking in concrete is modeled as a process of softening that begins with exceedance of the tensile strain capacity of concrete at $\varepsilon_t > \varepsilon_{ct}$ and is concluded at a smeared tangential tensile strain $\varepsilon_t = \varepsilon_u$, where ε_u corresponds to zero residual tensile strength. The smeared strains of ε_1 and ε_u in Fig. 3 are taken as $\varepsilon_1 = 0.0003$ and $\varepsilon_u = 0.002$, respectively [8].

Simple equilibrium conditions written along any radially cracked section give the following equation by introducing the softening behavior of concrete:

$$pR_0 = p_i R_i + \int_{R_0}^{R_i} \sigma_t \mathrm{d}r \tag{9}$$

where σ_t is the smeared tensile stress of the partly cracked inner part.

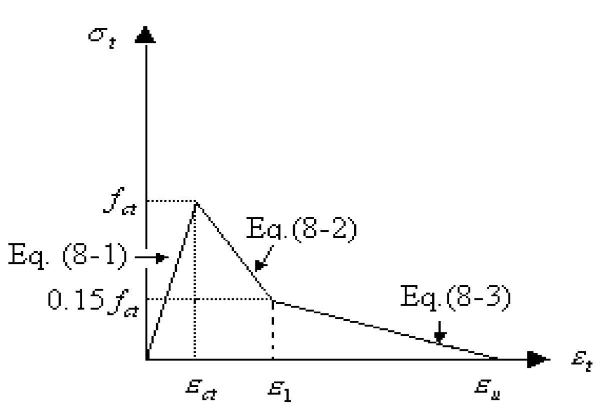

Fig. 3. Stress–strain curve of concrete in tension [8].

To solve the integral in Eq. (9), the relation between σ_t and ε_t must be considered. According to Eq. (7), the following equation can be obtained

$$\frac{\varepsilon_{t0}}{\varepsilon_{ct}} = \frac{R_i}{R_0} \tag{10}$$

where ε_{t0} is the smeared tangential strain at $r = R_0$.

Then, the following equation is obtained by introducing the relation between R_c and R_i:

$$\frac{\varepsilon_{t0}}{\varepsilon_{ct}} = \frac{R_i}{R_0} < \frac{R_c}{R_0} \tag{11}$$

Noticing that ε_{t0} lies in between ε_{ct} and ε_u, the integral in Eq. (9) can be obtained by considering Eq. (7), Eq. (11) and the relation between ε_{t0} and ε_1, ε_u:

$$\frac{R_i}{R_0} < \frac{R_c}{R_0} \le \frac{\varepsilon_1}{\varepsilon_{ct}},$$

$$I = \int_{R_0}^{R_i} \sigma_t \mathrm{d}r = \frac{f_{ct}}{\varepsilon_1 - \varepsilon_{ct}}\left[(\varepsilon_1 - 0.15\varepsilon_{ct})(R_i - R_0) - 0.85R_i\varepsilon_{ct}\ln\frac{R_i}{R_0}\right] \tag{12-1}$$

$$\frac{\varepsilon_1}{\varepsilon_{ct}} < \frac{R_i}{R_0} < \frac{R_c}{R_0} \le \frac{\varepsilon_u}{\varepsilon_{ct}}, \quad I = \int_{R_0}^{R_i} \sigma_t \mathrm{d}r = I_1 + I_2 \tag{12-2}$$

where

$$I_1 = \int_{R_0}^{RR_1} \sigma_t \mathrm{d}r = \frac{0.15 f_{ct}}{\varepsilon_u - \varepsilon_1}\left(\varepsilon_u\frac{R_i\varepsilon_{ct} - R_0\varepsilon_1}{\varepsilon_1} - R_i\varepsilon_{ct}\ln\frac{R_i\varepsilon_{ct}}{R_0\varepsilon_1}\right)$$

with $RR_1 = \dfrac{R_i\varepsilon_{ct}}{\varepsilon_1}$

$$I_2 = \int_{RR_1}^{R_i} \sigma_t \mathrm{d}r = \frac{f_{ct}}{\varepsilon_1 - \varepsilon_{ct}}\left[(\varepsilon_1 - 0.15\varepsilon_{ct})\frac{R_i(\varepsilon_1 - \varepsilon_{ct})}{\varepsilon_1} - 0.85R_i\varepsilon_{ct}\ln\frac{\varepsilon_1}{\varepsilon_{ct}}\right]$$

The case of $\varepsilon_u/\varepsilon_{ct} < R_i/R_0 < R_c/R_0$ is not considered because the bond failure in this case is a pullout-type failure, not a splitting-type failure [1,9].

Substituting Eqs. (3), (12-1) and (12-2) into Eq. (9), the radial pressure p is given by

$$pR_0 = R_i f_{ct}\frac{R_c^2 - R_i^2}{R_c^2 + R_i^2} + I \tag{13}$$

where I is given by Eqs. (12-1) and (12-2) according to different ratio of R_c/R_0.

Differentiation of Eq. (13) with respect to R_i gives

$$\frac{\mathrm{d}\left(\frac{pR_0}{f_{ct}}\right)}{\mathrm{d}R_i} = \frac{R_c^4 - R_i^4 - 4R_i^2R_c^2}{(R_c^2 + R_i^2)^2} + I' \quad (14)$$

where

$$\frac{R_i}{R_0} < \frac{R_c}{R_0} \le \frac{\varepsilon_1}{\varepsilon_{ct}},$$

$$I' = \frac{1}{\varepsilon_1 - \varepsilon_{ct}}\left[(\varepsilon_1 - 0.15\varepsilon_{ct}) - 0.85\varepsilon_{ct}\left(1 + \ln\frac{R_i}{R_0}\right)\right] \quad (14-1)$$

$$\frac{\varepsilon_1}{\varepsilon_{ct}} < \frac{R_i}{R_0} < \frac{R_c}{R_0} \le \frac{\varepsilon_u}{\varepsilon_{ct}}, \quad I' = I_1' + I_2' \quad (14-2)$$

where

$$I_1' = \frac{0.15}{\varepsilon_u - \varepsilon_1}\left[\frac{\varepsilon_u\varepsilon_{ct}}{\varepsilon_1} - \varepsilon_{ct}\left(1 + \ln\frac{R_i\varepsilon_{ct}}{R_0\varepsilon_1}\right)\right]$$

$$I_2' = \frac{\varepsilon_1 - 0.15\varepsilon_{ct}}{\varepsilon_1} - \frac{0.85\varepsilon_{ct}}{\varepsilon_1 - \varepsilon_{ct}}\ln\frac{\varepsilon_1}{\varepsilon_{ct}}$$

Putting Eq. (14) to zero and solving R_i numerically, the maximum pressure p_{max} can be obtained by taking the corresponding R_i into Eq. (13). As a result, bond stress between reinforcement and concrete can also be obtained.

3. Comparison with Tepfers' classic solution

The following notation is used for bar diameter and clear concrete cover thickness, respectively:

$$d = 2R_0 \qquad c = R_c - R_0 \quad (15)$$

The relative maximum pressure p_{max}/f_{ct} of the concrete ring as a function of the relative cover thickness c/d cal-

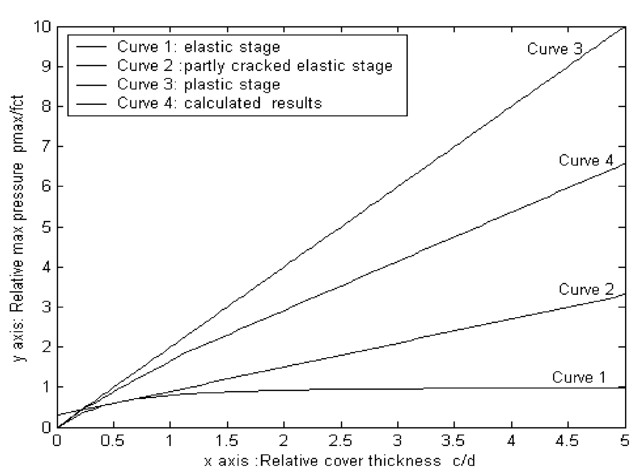

Fig. 4. The relative maximum pressure p_{max}/f_{ct} of the concrete ring as a function of the relative concrete cover thickness c/d in comparison with Tepfers.

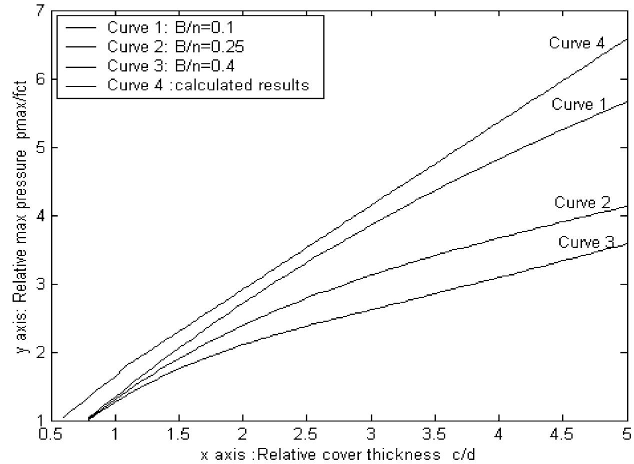

Fig. 5. The relative maximum pressure p_{max}/f_{ct} of the concrete ring as a function of the relative concrete cover thickness c/d in comparison with Nielsen.

culated by Eqs. (13) and (14) is given in Fig. 4. The three classic stages proposed by Tepfers [1] are also depicted in Fig. 4. It is seen from Fig. 4 that the calculated results approach the line for the plastic stage of Tepfers at lower values of c/d, while at larger values of c/d the calculated results lie in between the line for the partly cracked elastic stage and the plastic stage as pointed out by Tepfers.

4. Comparison with Nielsen's solution

An equivalent linear-elastic displacement field in the inner ring is assumed by Nielsen and Bicanic [7]. The brittleness number B (ratio between structural size and material characteristic size, given by $B = 2\pi R_0/l_{ch}$, where R_0 is the radius of the reinforced bar, l_{ch} is the characteristic length, defined originally by Hillerborg as $l_{cd} = E_0G_f/f_{ct}^2$, where G_f is the fracture energy of concrete) and the number of radial crack n are introduced. The solution depends on the ratio B/n. The relative maximum pressure p_{max}/f_{ct} as a function of the relative cover thickness c/d for three different values of B/n is depicted in Fig. 5, comparing with those calculated by Eqs. (13) and (14). It can be seen from Fig. 5 that the line for Nielsen's results for $B/n = 0.1$ (smaller values B/n give more plastic behavior in the inner ring) approach the line for the calculated results, while for larger ratio B/n, such as $B/n = 0.4$, the difference between Nielsen's results and the calculated results is clearly seen in Fig. 5. The advantage of the present analytical model is evident because the results of the problem are independent of the choice of the number of radial crack n.

5. Conclusion

An analytical model to predict the carrying capacity of a thick-walled cylinder exposed to internal radial pressure is proposed. The methodology suggested by Tepfers without including softening behavior of concrete is used to determine the effect of concrete confinement of cover thickness on the bond strength between ribbed reinforcement and concrete, including the residual strength of the concrete cover after its tensile capacity of concrete is exceeded. The concepts of smeared cracking and average stress–strain relationship of concrete in tension are introduced to consider the softening behavior of concrete.

The analytical solution is compared with Tepfers' classic solution and Nielsen's solution. The results fall in between the partly cracked elastic stage and the plastic stage of Tepfers' solution as anticipated by Tepfers. For smaller ratio B/n, such as $B/n = 0.1$, Nielsen's results approach the solution calculated by Eqs. (13) and (14), while for larger ratio B/n, such as $B/n = 0.4$, the two results are different. The advantage of the present model is clear because the results of the problem are independent of the choice of the number of radial crack n.

Acknowledgements

This paper is supported by the National Key Basic Research and Development Program (973 Program) no. 2002CB412709.

References

[1] R. Tepfers, Cracking of concrete cover along anchored deformed reinforcing bars, Mag. Concr. Res. 31 (106) (1979) 3–12.
[2] H.W. Reinhardt, C. Van Der Veen, Splitting failure of a strain-softening material due to bond stresses, in: A. Carpinteri (Ed.), Applications of Fracture Mechanics to Reinforced Concrete, Elsevier, Amsterdam, The Netherlands, 1992, pp. 333–346.
[3] T. Olofsson, K. Noghabai, U. Ohlsson, L. Elfgren, Anchorage and bond properties in concrete, in: G. Baker, B.L. Karihaloo (Eds.), Fracture of Brittle, Disordered Material-Concrete, Rock and Ceramics, E&FN Spon, Chapman & Hall, UK, 1995, pp. 525–543.
[4] K. Noghabai, Environmental effects on bond in reinforced concrete structures, in: C.S. Jöström (Ed.), Durability of Building Materials and Components 7 (Volume One), Proceedings of the 7th International Conference, Stockholm, Sweden, May, E&FN Spon, Chapman & Hall, UK, 1996, pp. 605–614.
[5] P.G. Gambarova, G.P. Rosati, C. Schumm, An elasto-cohesive model for steel–concrete bond, in: Z.P. Bazant, Z. Bittnar, M. Jirásek, J. Mazars (Eds.), Proceedings of the Europe–US Workshop on Fracture and Damage in Quasibrittle Structures, Prague, E&FN Spon, Chapman & Hall, UK, 1994, pp. 557–566.
[6] P.G. Gambarova, G.P. Rosati, Bond and splitting in bar pull-out: behavioural laws and concrete cover role, Mag. Concr. Res. 49 (179) (1997) 99–110.
[7] C.V. Nielsen, N. Bicanic, Radial fictitious cracking of thick-walled cylinder due to bar pull-out, Mag. Concr. Res. 54 (3) (2002) 215–221.
[8] S.J. Pantazopoulou, K.D. Papoulia, Modeling cover-cracking due to reinforcement corrosion in RC structures, J. Eng. Mech. 127 (4) (2001) 342–351.
[9] J. Cairns, K. Jones, An evaluation of the bond-splitting action of ribbed-bars, ACI Mater. J. 93 (1) (1996) 10–19.